NORMAL FREEZING OF ORGANIC LIQUIDS

by

DAVID ARTHUR IRVIN

B.S., San Jose State College, 1964

———————

A MASTER'S THESIS

submitted in partial fulfillment of the
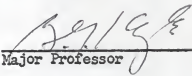
requirements for the degree

MASTER OF SCIENCE

Department of Chemical Engineering

KANSAS STATE UNIVERSITY
Manhattan, Kansas

1965

Approved by:

Major Professor

TABLE OF CONTENTS

A	a constant of integration
b	dimensionless boundary layer thickness ($\delta f/D$)
B	a constant of integration
C	solute concentration in liquid at distance x from interface, moles/volume
C_a	solute concentration in liquid at equilibrium with solid phase, moles/volume
C_e	eutectic composition, moles/volume
C_L	bulk liquid concentration, moles/volume
C_o	initial solute concentration in liquid, moles/volume
C_s	solute concentration in solid at equilibrium, moles/volume
D	coefficient of diffusion
e	base of natural logarithm
f	rate of freezing (distance/time)
g	fraction frozen
g_o	fraction frozen of pure component
G	temperature gradient in liquid
k	a constant
K_E	effective distribution coefficient
K_o	equilibrium distribution coefficient
L	moles of liquid
L_o	initial moles of liquid
m	slope of liquidus line
n	dimensionless distance from interface into liquid
q_o	fraction frozen of pure component

s   moles of solute remaining in the system after a certain degree of solidification

s_o total moles of solute in the system

T_E equilibrium temperature

T_o initial temperature

W_e weight fraction of solute in eutectic

W weight fraction in liquid a distance x from interface

W_ℓ mean bulk weight fraction in liquid

W_s weight fraction of solid

W_o initial weight fraction in liquid

x distance from initial point of freezing

x' distance from interface

$\bar{x}_o$ initial mole fraction of liquid phase

$\bar{x}$ mole fraction of liquid phase

α Kf/D

δ boundary layer thickness

ϵ dimensionless eutectic composition

Φ W/W_o

Φ_ℓ W_ℓ/W_o

INTRODUCTION

Normal freezing is a term applied to the progressive freezing of a liquid charge. It is well known that when a solution undergoes a normal freezing process a nonlinear composition profile will result.

The first quantitive explanation of this phenomena was developed by Pfann (1). Historically, normal freezing has been applied to the purification of materials exhibiting solid solution phase behavior; therefore, Pfann approximated the solid solution phase diagram with straight lines as shown in Figure 1. From thermodynamics it can be shown that this approximation becomes better as the solute concentration decreases. The assumption of low solute concentration is not a serious restriction as usually normal freezing is applied to just such cases. It is convenient to define the equilibrium distribution coefficient as shown below.

$$K_o = c_s/c_a$$

This coefficient can be considered a constant because of the straight line assumption made for the phase diagram. Other assumptions made by Pfann are:

1. Diffusion of solute in the solid is negligible

2. Mixing in the liquid phase is complete.

By definition

$$C_s = K_o C_a \qquad (1)$$

The liquid phase composition is given by

$$C_a = s/(1-g) \qquad (2)$$

Combining Equations (1) and (2)

$$C_s = K_o s/(1-g) \qquad (3)$$

assuming freezing to take place in a tube of unit volume. Let an element of

volume dg freeze. The concentration of this frozen volume is:

$$C_s = -ds/dg \tag{4}$$

Eliminating C_s from Equation (3) and expressing as an integral:

$$\int_{s_o}^{s} \frac{ds}{s} = - K_o \int_{0}^{g} dg/(1-g) \tag{5}$$

Integrating:

$$s = s_o \, (1-g)^{K_o} \tag{6}$$

Eliminating s by using Equation (3) and noting that $C_o = s_o$

$$C_s = K_o C_o (1-g)^{Ko} \tag{7}$$

This is Pfann's expression for solute distribution in a solid when the liquid phase is completely mixed.

Tiller, Jackson, Rutter, and Chalmers (2) have derived the expression for solute distribution assuming that liquid phase mixing is negligible and mass transfer is caused only by diffusion. As in Pfann's analysis, solid phase diffusion is assumed to be negligible and K_o is assumed to be constant. For sake of analysis the freezing is assumed to take place uniaxially in a tube of unit cross-section. As freezing occurs solute is rejected by the solid and diffuses into the liquid causing a build up os solute in the liquid near the interface and hence a concentration gradient. A sketch of this concentration gradient is presented in Figure 2. The rate of freezing will be constant and equal to f. Assuming steady state, the flows into and out of the liquid volume element dx are:

Flow into element

Bulk Flow $\qquad f \left[C + (\frac{dC}{dx}\text{'}) \; dx\text{'} \right]$

Diffusion $\qquad - D \frac{dC}{dx}\text{'}$

Flow out of element

    Bulk flow fC

    Diffusion $- D \left[\dfrac{d}{dx'} \left(C + \left(\dfrac{dC}{dx'}\right) dx' \right) \right]$

Assuming no accumulation

    Flow in - flow out = 0

$$f \left[C + \left(\frac{dC}{dx'}\right) dx' \right] - D \frac{dC}{dx'} - fC + D \left[\frac{dC}{dx'} + \frac{d}{dx'} \left(\frac{dC}{dx'}\right) dx' \right] \quad (8)$$

Simplification gives:

$$f \frac{dC}{dx'} + D \frac{d^2 C}{dx'^2} = 0 \quad (9)$$

The boundary conditions are:

     $x' \quad \infty \quad\quad C_L = C_o$

     $x' = 0 \quad\quad C_L = C_o / K_o$

The solution is then:

$$C_L = A\, e^{- \frac{fx'}{D}} + C_o \quad (10)$$

For steady state it is necessary that $C_s = C_o$, also it is apparent that:

$$A = C_o / K_o - C_o \quad (11)$$

combining Equations (10) and (11):

$$C_L = C_o \left[1 + \frac{1 - K_o}{K_o} e^{- \frac{fx'}{D}} \right]$$

This is the composition profile as it exists in the liquid phase. Since we desire the solid phase profile our analysis is not complete. Figure 3 shows a sketch of what the distribution profile should look like if it followed the expected general conditions.

1. The initial solidification would have a value of $K_o C_o$

2. C_o should be approached asymptotically as the liquid phase disappears.

3. C_s must rise continuously from $K_o C_o$ to C_o from a solute material balance it is seen, Figure 3, that the area between C_o and C_s curves must equal the area between the C_L and C_o curves. This can be re-presented analytically as Equation (13).

$$\int_0^x {}^\infty (C_o - C_s)\ dx = \int_x^{x'} {}^\infty (C_L - C_o)\ dx'$$ (13)

If it is assumed that the rate of approach of C_s to C_o with distance is proportional to $(C_o - C_s)$, then:

$$\frac{d(C_o - C_s)}{dx} = -\alpha(C_o - C_s)$$ (14)

Equation (14) satisfies the above set of conditions. The solution to this equation is:

$$C_o - C_s = A\ e^{-\alpha x} + B$$ (15)

applying the previously mentioned conditions:

$$(C_o - C_s) \quad 0 \qquad\qquad x \quad \infty$$
$$C_s = K_o C_o \qquad\qquad x = 0$$

the solution is:

$$C_s = C_o \left[1 - (1 - K_o)\ e^{-\alpha x}\right]$$ (16)

substituting Equations (12) and (16) into (13) gives:

$$C_o(1 - K_o) \int_0^\infty e^{-\alpha x}\ dx = C_o \frac{1 - K_o}{K_o} \int_0^\infty e^{-\frac{fx'}{D}}\ dx'$$ (17)

This equation yields

$$\alpha = \frac{K_o f}{D} \tag{18}$$

using this value of α, Equation (16) becomes:

$$C_s = C_o \left[1 - (1-K_o) \exp \left(-\frac{K_o f}{D} x \right) \right] \tag{19}$$

The derivation of this equation makes no provision for the excess of solute that will appear in the terminal region and therefore, cannot be applied to the final stages of solidification. It has been shown by Smith, Tiller and Rutter (3) that the terminal transient will appear as shown in Figure 4. The equation for the terminal transient is quite cumbersome and will not be included here.

The first two equations (7) and (19) represent extremes in the assumed liquid phase mixing. The analysis by Burton, Prim and Slichter (4), represents the condition of partial mixing by using a boundary layer approach. Using Equation (9) and applying the boundary condition:

$$C = C_o \qquad \text{at} \qquad x' = \delta$$

This assumes that the concentration gradient exists only in a boundary layer of thickness δ and that outside the boundary layer the concentration is C_L. From the steady state analysis it is seen that another boundary condition is:

$$(C_a - C_s) f + D \frac{dC}{dx'} = 0 \qquad \text{at} \qquad x' = 0 \tag{20}$$

applying these boundary conditions to Equation (9) gives:

$$\frac{C_o - C_s}{C_a - C_s} = e^{-f\delta/D} \tag{21}$$

Defining a new variable K_E

$$K_E = C_s / C_o$$

called the effective distribution coefficient and substituting K_o and K_E into Equation (21) gives in logarithmic form.

$$\ln \left(\frac{1}{K_E} - 1\right) - \ln \left(\frac{1}{K_o} - 1\right) = -\frac{f\delta}{D} \tag{22}$$

This is the working form of the equation used in this investigation. Notice this equation is consistent with the extreme cases of no mixing and complete mixing:

No mixing ---------- $f = \infty$ and $K_E = 1$

complete mixing ----- $f = 0$ and $K_E = K_o$

The qualitative representation of solute distribution along the growth axis is represented in Figure 5, for the three cases discussed here. It is seen that Pfann's complete mixing model gives the best segregation while the no-mixing model of Tiller et. al. gives the poorest segregation. Therefore, mixing of the liquid phase would be expected to increase segregation.

All the previous discussion has concerned mixtures having solid solution phase behavior. However, this thesis is concerned with binary organic systems which in general exhibit simple eutectic phase behavior. A typical phase diagram for such an organic system is shown in Figure 6. Notice that the solid phase obtained from an organic mixture of composition C_o would be expected to consist of pure component A, in other words the value of K_o is zero. This means that technically the previous equations applying to solid solutions are not applicable to eutectics as a review of the derivations will show.

For complete mixing of a liquid phase, simple eutectic-forming mixture the analysis is easy. Pure solute will freeze out until the liquid phase reaches the eutectic composition; then the solid phase will freeze at the eutectic composition, see Figure 7.

Wilcox (5) has analysed and obtained an equation for simple eutectic-forming mixtures assuming a boundary layer exists next to the interface in which no mixing occurs, the bulk of the liquid is assumed well mixed.

According to Wilcox, a certain fraction of liquid will freeze producing pure component in the solid phase. The expression for this fraction is:

$$q_o = (\epsilon e^{-b} - 1) / \epsilon e^{-b} \tag{23}$$

When more than this fraction of liquid is solidified the eutectic composition is reached in the boundary layer and the distribution is given by Equation (24)

$$W_s = W_e \left\{ 1 - \left[\frac{(1-g)}{(1-g_o)} \right] \exp (e^{-b}/1 - e^{-b}) \right\} \tag{24}$$

Figure 8 shows the calculated solute profile obtained by applying Wilcox's equations to a hexadecane-benzene system containing 3 mole % hexadecane.

Past experimental work with solid solutions has shown the actual segregation to be less than that predicted by theory. The chief reason for this lack of verification is thought to be due to a phenomenon first proposed by Rutter and Chalmers (6) termed "constitutional subcooling". As the interface of a freezing solution rejects solute a concentration gradient will exist in the liquid as already shown in Figure 2. Since the equilibrium freezing temperature depends upon concentration (as determined by the phase diagram), an equilibrium temperature gradient will exist similar to curve "a" of Figure 9. The actual temperature gradient imposed in the liquid can be represented by curve "b". At every point where curves "b" is below curve "a" the liquid will be subcooled. By representing curves "a" and "b" analytically, Tiller, et al. (2) were able to show that the critical rate above which subcooling will exist is given by:

$$f = - \frac{GD}{(\frac{mC_o}{K_o}) (1-K_o)} \tag{25}$$

This equation implies that there is a minimum rate of freezing below which no subcooling will exist. This then is the phenomena known as constitutional

supercooling and is responsible for the irreularities observed at the inter-
face of freezing mixtures.

PROCEDURE

The apparatus used for conducting normal freezing experiments consisted of a refrigerated methyl alcohol bath and a drive mechanism to control freezing rates. The bath temperature was varied from -10 C to -33 C for different runs, and was controlled so that the maximum variation for any temperature setting was approximately one degree. To keep the bath at a uniform temperature it was agitated by a 1/12 H. P. Fultork Labmotor operating a stirrer.

The drive mechanism consisted of a long upright shaft threaded to screw into a threaded gear. Keeping the gear stationary in the horizontal plane and allowing the gear to rotate caused the shaft to ascend or descend depending on the direction of rotation. A rachet assembly powered by a 1/30 H. P. motor caused the gear to rotate. The rod could descend at a constant rate between 0.1 in./hr. and 3.0 in./hr. depending on the rachet setting. The drive was equipped with an automatic shut off to stop the motor at the completion of each run. To allow the motor to run might damage the drive mechanism.

In making a typical experimental run a glass tube sealed at one end was filled with approximately 50 grams of the specimen solution. The weight of the specimen was recorded as a mass balance check. The tube was held in place vertically over and just touching the bath by means of a clamp attached to the descending rod. The motor was started and the tube slowly descended into the bath. Usually it would take several minutes for the liquid to start freezing. If freezing had not occurred in the first several minutes the tube was tapped gently so as to initiate the freezing. After the entire specimen had frozen the drive was stopped.

In order to determine the composition profile it was necessary to divide the solid specimen into a number of portions, (usually eight). Removal of each portion was accomplished by raising the tube out of the bath so the volume of solid to be removed was above the level of the bath, this portion was then allowed to melt. Generally a half hour was required to complete the melting of each portion. Care was exercised at this point as the interface tends not to be flat. Upon standing a time, (depending on tube diameter) the interface became flat. Only a melt with a flat interface will give an accurate composition measurement. Each melted portion was transferred to a weighing bottle and weighed to a 1/10 milligram.

A Bausch and Lomb refractometer was used to measure the refractive index of each increment. A composition curve versus refractive index had been determined from mixtures of known composition and was used to convert refractive indexes to compositions. All the refractive indexes were read at 25.0 °C to an accuracy of $\pm$ 0.0001. The calibration curve for the hexadecane-benzene system is given in appendix (1).

Three liquid systems were investigated, they were:

>benzene-normal heptane
>
>benzene-cyclohexane
>
>benzene-hexadecane

All starting mixtures of benzene-hexadecane contained approximately 97 mole % benzene. The heptane system contained 98 mole % benzene while the cyclohexane system contained 96 mole % benzene.

For some runs it was necessary to remove dissolved gas from the specimen. This was accomplished by submerging the entire tube in the bath until the contents has become solid, then evacuating the tube and allowing the solid

to melt. When this process was repeated three times the specimen was effectively degassed and no bubble formation during normal freezing was observed. To be certain the degassing process did not redistribute the solute the liquid was carefully agitated before each run.

Mixing of the liquid portion of the sample during freezing was accomplished by attaching a flat disc to a line and suspending the disc horizontally in the liquid phase. Allowing the disc to reciprocate up and down, by means of a motor, caused mixing in the liquid phase. This arrangement was used in favor of a blade stirrer as the amount of agitation caused by a stirrer is dependent upon the amount of liquid, (constantly changing during a run). The mixing caused by the chosen arrangement was considered to be independent of the quantity of liquid.

To obtain temperature distributions during freezing a thermocouple was suspended in the liquid at a fixed distance relative to the tube. As the solid-liquid interface moved up the tube, temperature measurements were taken at various times so that a temperature profile was obtained. The point at which the interface touched the thermocouple was recorded. Temperatures were read to an accuracy of 0.05 °C.

In order to better understand the solute rejection mechanism photographic studies were made of the solid-liquid interface. A microscope equipped with a camera was mounted a few degrees above the horizonal position. With this arrangement a profile microphotograph of the interface could be obtained. In order to prevent distortion the interface was photographed in a tube with polished flat slides. All photographs were made at the same magnification of 14 times. Exposure time was 15 seconds; this long exposure time required that the drive mechanism be stopped just prior to exposure to insure against

movement of the tube. A fine grain film (Kodak Contrast Process Ortho) was used for all photographs and developed with a high contrast developer (Kodak D-11).

RESULTS

The effect of the following parameters on segregation by normal freezing was investigated.

1. Bath temperature.

2. Mixing of liquid phase.

3. Degassed specimen.

4. Tube diameter.

It was found that each individual run was well represented by the incomplete mixing model. Figures 10, 11, 12 and 13 are typical of the composition profiles obtained. Wilcox's equations for eutectic systems were found not to apply as at no time was 100 % pure material obtained. Equation (7) for the incomplete mixing model can be put in the following form.

$$\ln \bar{x}/\bar{x}_o = (1 - K_E) \ln L_o/L \qquad (26)$$

It was found that a log-log plot of x/x_o versus L_o/L for all runs was represented well with a straight line. Figures 14 and 15 are typical of this correlation. Because of the excellent agreement it was possible to calculate K_E from the slopes of these plots. Table 1 contains values of the distribution coefficient for all runs. In order to correlate K_E and f, Burton, Prim, and Slichter's boundary layer model was employed. From Equation (22) it is seen that a semi-log plot of $(1/K_E - 1)$ versus f would be expected to produce a straight line of slope - δ/D and intercept of $(1/K_o - 1)$. Previously it was found, (7) that this correlation applied well to the cyclohexane-benzene and heptane-benzene systems as shown in Figures 16, 17, and 18. The hexadecane-benzene system, Figures 19, 20 and 21 were best represented by two straight lines. However, a single straight line was found to fit the stirred and degassed runs, Figures 22 and 23.

Effect of Parameters

Bath temperature

The effect of bath temperature on nonstirred runs can be seen from Figure 20. Five data points were taken for a low -30 °C bath temperature and seven points were taken at a higher -18 °C bath temperature. It is seen that over this temperature range, bath temperature appears to have no effect on segregation. Figure 22 shows the effect of bath temperature on a stirred system; it is seen that segregation for the hexadecane-benzene system decreases with decreasing bath temperature.

Mixing of liquid phase

For the cyclohexane-benzene system it was found that mechanical stirring of the liquid phase increased segregation as illustrated in Figure 24. However, Figure 25 shows that similar stirring of the hexadecane-benzene system produced less segregation than was obtained for unstirred runs.

Degassed specimen

All runs produced gas bubbles at the interface except when the specimen was purposely degassed as mentioned in the procedure. The effect of gas bubbles was investigated only for the hexadecane-benzene system. Figure 26 shows that removal of the dissolved gas decreased segregation.

Tube diameter

The effect of tube diameter was investigated for the hexadecane-benzene system. Figure 27 is a summary of the results that were presented in Figures 19, 20, and 21. It is seen that segregation increases with increasing tube diameter.

Photographic Studies

Microphotographs were taken of the interface of pure benzene and the hexadecane-benzene system. These photographs are presented as plates (1) through (5). It is observed that at freezing rates between 1.0 and 2.5 in./hr. the interface maintains an irregular dendritic surface. At freezing rates less than 1.0 in./hr. the interface shows a change from dendritic formation to a more regular but corrugated surface.

It was difficult to photograph the interface of pure benzene as this substance is not opaque when frozen, as is the hexadecane-benzene system, but remains clear. Plate (6) is the best photograph that could be obtained for pure benzene. The interface is faint but discernible as a sharp line across these photographs. The white blotches in the background above the interface are reflections from bubbles still attached to the interface.

Constitutional Subcooling

Temperature profiles were taken in order to solve Equation (25) and to determine if constitutional subcooling was occuring. A typical profile is presented in appendix (2). The rate of freezing was found to have a small effect on the temperature gradient. Equation (25) revealed that all runs were subject to constitutional subcooling effects.

DISCUSSION

Bath temperature

It might be expected that bath temperature would not effect segregation as the position of the interface relative to the bath level will vary so that the interface is at the freezing temperature and not necessarily at the bath temperature. This was found true for unstirred runs. The effect of bath temperature on stirred runs is thought to be due to the rather high eutectic temperature, (see appendix 3) of the hexadecane-benzene system. It was observed that for the same bath temperature the interface for stirred runs was significantly lower relative to the bath than for unstirred runs. This suggests that the interface is not at the equilibrium temperature, but is below this temperature. For the hexadecane-bezene system if the interface temperature were only a few degrees below the equilibrium temperature it would be possible to freeze liquid at the eutectic composition resulting in lowered segregation.

Mixing of liquid phase

Mixing of the liquid phase for the cyclohexane-benzene system improved segregation as expected, since the eutectic temperature for this system is well below the bath temperature. The reason for decreased segregation of the stirred hexadecane-benzene system is believed to be due to the high eutectic point of this system as mentioned above.

Degassed specimen

The decrease in segregation caused by degassing of the specimen is in keeping with the boundary layer theory. It would be expected that rising bubbles of gas would cause a certain degree of mixing to occur in the liquid.

Since mixing increases segregation, the removal of the source of this mixing should cause a drop in segregation. It should be pointed out that this conclusion is not necessarily inconsistent with the lack of separation observed in the stirred system as the agitation caused by rising gas bubbles is very mild compared to the vigorous forced convection caused by the stirrer. The interface distance was not observed to change because of degassing, indicating the effect of nonequilibrium freezing was not present.

Tube diameter

Perhaps the strongest support for the boundary layer model is found in the effect of tube diameter on segregation. From elementary boundary layer theory it is known that as convection in a fluid increases the stagnant boundary layer decreases. Also increasing tube diameter would be expected to result in an increase of natural convection. As shown in the results the largest diameter tube gave the better segregation at a particular freezing rate and the smallest tube gave the poorest segregation. Furthermore, it was noticed that for rates less than 1.0 in./hr. the smallest tube size had the greatest slope, Figure 27 while the largest tube had the least slope. The slope of these lines as given by Equation (22) is $-\delta/D$. If it is assumed that D remains unchanged then δ must decrease as the tube size increases, thus satisfying the above mentioned expectations. The branch of the hexadecane line, Figure 27 for rates greater than 1.0 in./hr. does not satisfy the requirement that the smallest tube should give the greatest slope, this may be explained as follows.

Constitutional subcooling

The interface of the hexadecane-benzene system was found to possess an

irregular surface. However, the microphotographs reveal a change in the type of surface irregularities occurring at a rate of 1.0 in./hr.. For rates is excess of 1.0 in./hr. the interface becomes quite dendritic, see Plates (4) and (5). It is believed that the discontinuous slope for the hexadecane-benzene curve shown in Figure 27 is a direct consequence of this change of interfacial morphology. Both changes appear to occur at a freezing rate of 1.0 in./hr.. The nature of the dendritic interface is such that it would appear that trapping of liquid could readily occur for freezing rates greater than 1.0 in./hr.. Any trapping of liquid would be expected to lessen the degree of segregation and hence a change in slope of the line in Figure 24. For freezing rates less than 1.0 in./hr. the interface took on a more corrugated appearence, Plates (1), (2) and (3). The amount of liquid trapping for this type of interface would be expected to be much less than for the dendritic interface. Nevertheless some degree of liquid trapping could be expected, thus accounting for the non-zero equilibrium distribution coefficients obtained as the exprapolated intersection of the plot of Figure 24. at zero freezing rate. This transition from a corrugated to a dendritic interface is believed to be analogous to the transition from a celluar interface to a dendritic interface as observed in metal systems by other investigators (8), (9), and (10).

Furthermore, the better segregation obtained for the cyclohexane-benzene and the heptane-benzene systems is believed to be due to a celluar rather than a dendritic interface for these systems over the freezing rates investigated. It can be shown that the transition from a celluar to a dendritic interface would be expected at a lower freezing rate for the hexadecane-benzene system. Both the solid solution and eutectic boundary layer models

account for this fact. For solid solutions Equation (25) gives the critical value of f above which subcooling occurs. This can be rearranged to:

$$\frac{D}{f} = \frac{mC_0}{GK_0}(1 - K_0)$$ (27)

Using Wilcox's equations for eutectic systems the critical f is given by, appendix (4):

$$\frac{G}{mC_\ell} = (\frac{\delta}{D}) \; e^{\; \delta(f/D)}$$ (28)

All factors in Equations (26) and (27) are constant except D and f; However, the ratio D/f must also be constant, therefore:

$$D = kf$$ (29)

Strictly speaking Equations (27) and (28) apply only at the transition from a flat interface to a cellular interface; however, similar considerations would be expected to be valid at the transition of a cellular to a dendritic interface. The table below shows the values of D, (11).

	$D \; (cm^2/sec)$	$\delta \; (cm)$
cyclohexane-benzene	1.36×10^{-5}	4.2×10^{-3}
heptane-benzene	1.13×10^{-5}	4.2×10^{-3}
hexadecane-benzene	0.70×10^{-5}	4.7×10^{-3}

Because of the lower diffusion coefficient the transition would be expected to occur at a lower freezing rate for the hexadecane-benzene system.

As assumed above and as expected from boundary layer theory the boundary layer thickness should be independent of the nature of the solute and of the freezing rate. The above table shows δ as calculated from the slope of the curves in Figures 16, 18, and 20 and from the value of D. The boundary layer thickness appears to be relatively constant, thus adding support to the boundary layer theory.

CONCLUSIONS

The variation of segregation by normal freezing with freezing rate
is well represented by Burton, Prim and Slichter's incomplete mixing boundary
layer model. The effects of mixing, tube diameter and bath temperature can
be explained in terms of this boundary layer model. The failure of Wilcox's
model for eutectic systems is thought to be due to constitutional subcooling
which in turn results in the trapping of liquid in the solid.

Table 1

Run No.	Freezing Rate (in./hr.)	Distribution Coefficient	Bath Temperature
	Hexadecane-Benzene	3/4" Dia. Tube	
1	2.25	.733	- 20
4	1.75	.721	- 20
5	1.25	.668	- 20
6	.75	.648	- 20
7	3.0	.807	- 20
8	.50	.623	- 20
9	1.75	.717	- 33
11	2.75	.789	- 33
12	.50	.437	- 33
13	.75	.627	- 33
14	.50	.607	- 33
68	.25	.525	- 20
71	.10	.485	- 20
	Hexadecane-Benzene	1.0" Dia. Tube	
22	1.75	.684	- 20
23	2.75	.716	- 20
36	2.5	.709	- 20
37	1.75	.694	- 20
38	1.25	.635	- 20
39	.75	.635	- 20
42	3.0	.714	- 20

Table 1 cont'd

Run No.	Freezing Rate (in./hr.)	Distribution Coefficient	Bath Temperature
43	1.0	.636	– 20
69	.25	.538	– 20
	Hexadecane-Benzene	1/2" Dia. Tube	
57	2.75	.771	– 20
58	2.75	.785	– 20
59	2.0	.747	– 20
60	1.0	.689	– 20
61	1.5	.760	– 20
62	.50	.593	– 20
63	2.75	.799	– 20
64	.75	.641	– 20
65	1.25	.717	– 20
66	1.00	.676	– 20
67	.25	.520	– 20
	Degassed Hexadecane-Benzene	3/4" Dia. Tube	
41	3.0	.758	– 20
40	1.75	.756	– 20
45	1.75	.796	– 20
46	1.75	.829	– 20
47	1.75	.795	– 20
48	2.75	.859	– 20
49	2.75	.860	– 20

Table 1 cont'd

Run No.	Freezing Rate (in./hr.)	Distribution Coefficient	Bath Temperature
50	.75	.760	- 20
51	1.25	.711	- 20
52	1.25	.802	- 20
53	1.0	.810	- 20
54	.50	.753	- 20
55	.50	.708	- 20
56	.50	.715	- 20
	Stirred Hexadecane-Benzene 3/4" Dia. Tube		
17	2.75	.809	- 18
18	.50	.681	- 18
19	1.75	.757	- 18
20	.75	.698	- 18
21	2.25	.790	- 18
15	1.25	.8105	- 28
16	2.00	.8125	- 28
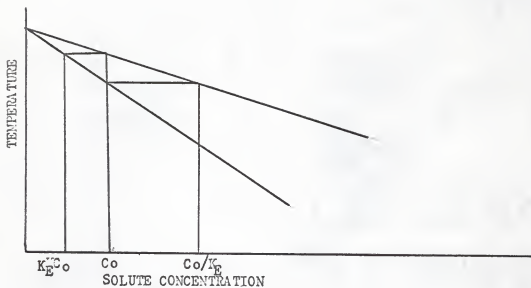
Fig. 1.   Portion of solid solution phase diagram.
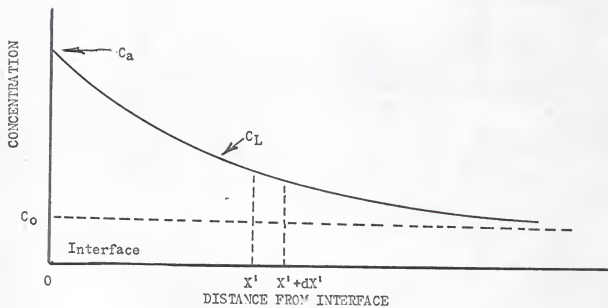
Fig. 2.   Distribution of solute ahead of interface.
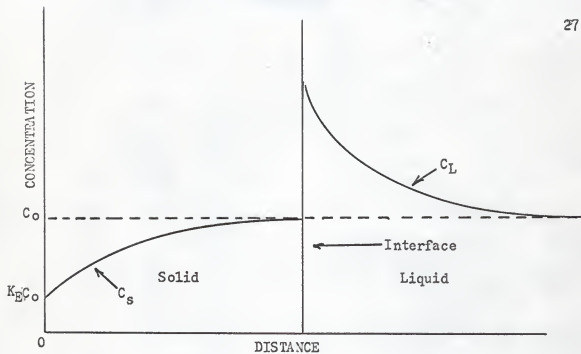
Fig. 3. Distribution of solute in solid and liquid phases.
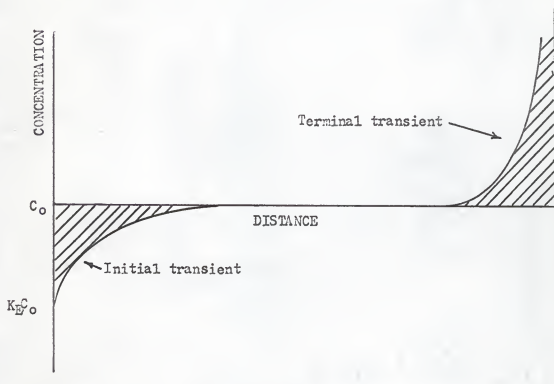
Fig. 4. Concentration profile of frozen specimen.
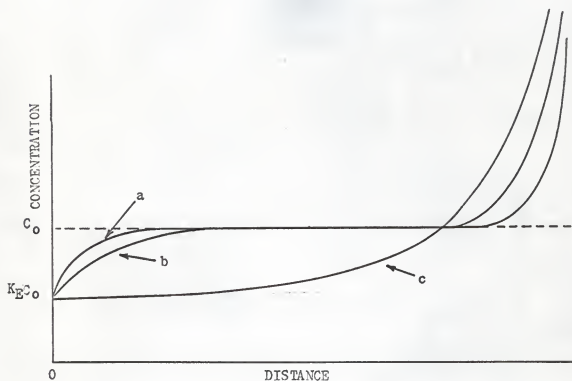
Fig . 5. Solute distribution along growth axis.

a) NO MIXING IN LIQUID
b) PARTIAL MIXING IN LIQUID
c) COMPLETE MIXING IN LIQUID
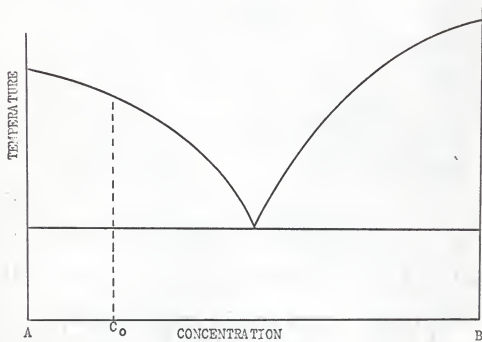
Fig . 6. Typical simple eutectic phase diagram.
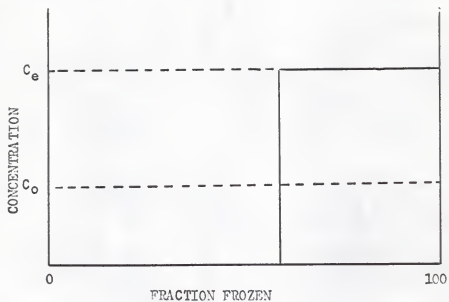
Fig. 7. Solute distribution profile of simple eutectic forming mixture.
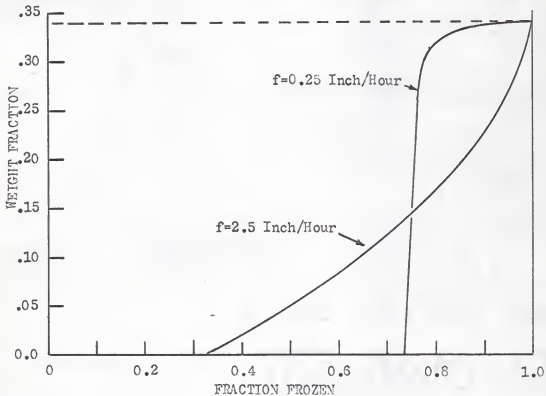
Fig. 8. Calculated solute distribution using Equation (22) for 3 mole % hexadecane and benzene.
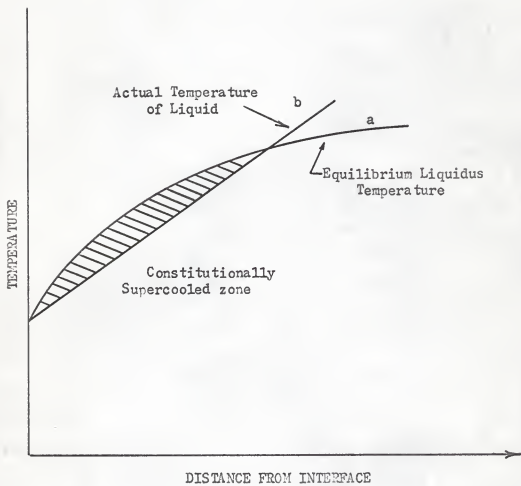
Fig . 9. Constitutionaly supercooled zone ahead of interface.
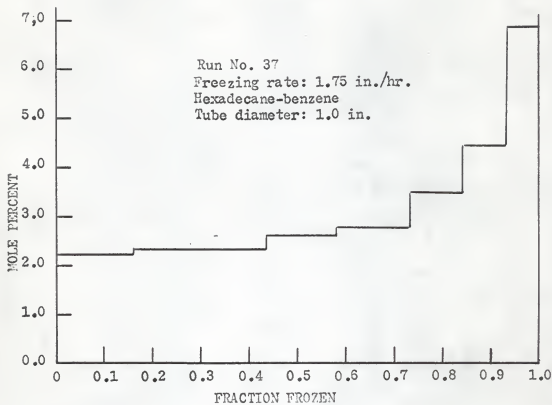
Fig. 10.   Composition profile.
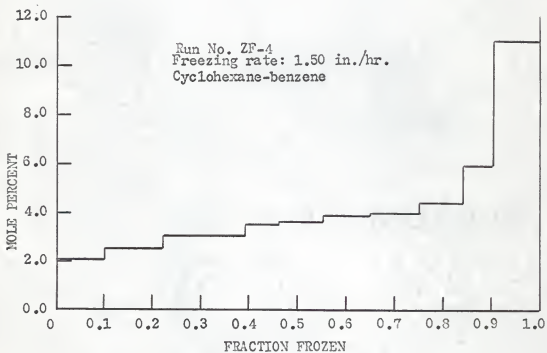
Fig. 11.   Composition profile.
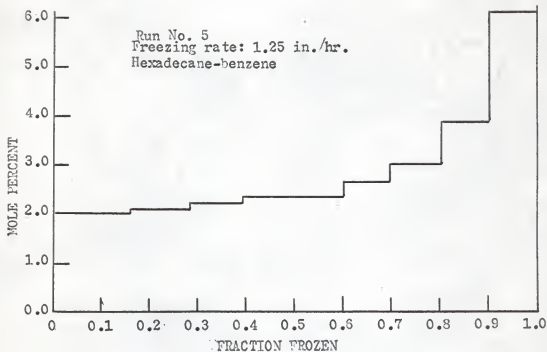
Fig. 12.   Composition profile.
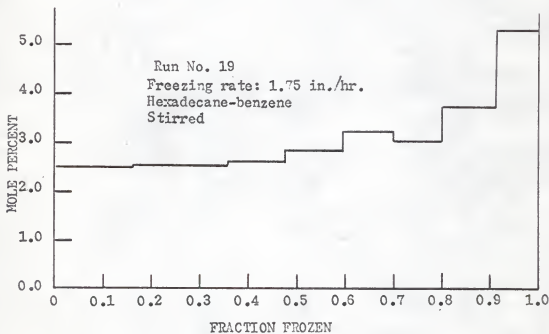
Fig. 13.   Composition profile.
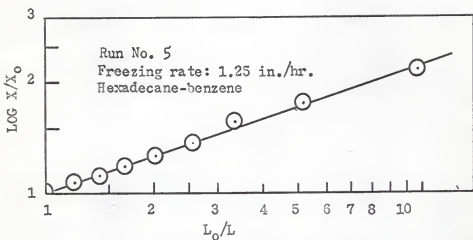
Fig. 14.   LOG X/X_0 versus LOG L_0/L.
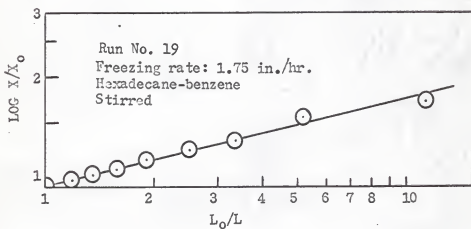
Fig. 15.   LOG X/X_0 versus LOG L_0/L.
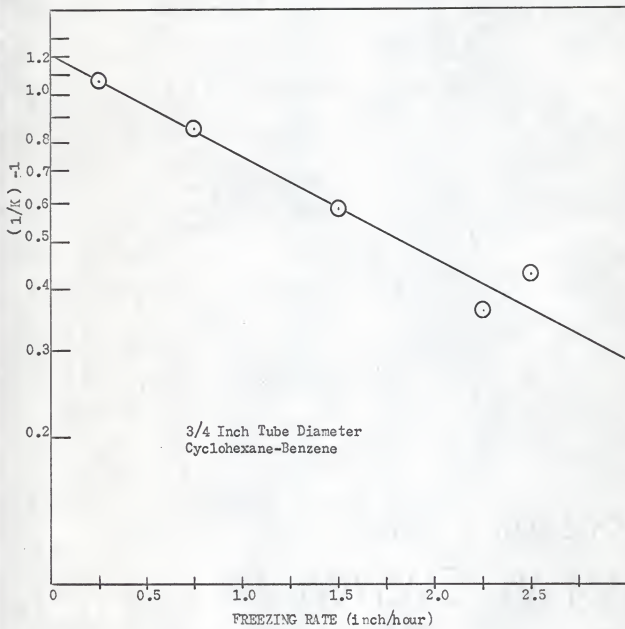
Fig. 16. LOG((1/K$_E$) -1) versus freezing rate.
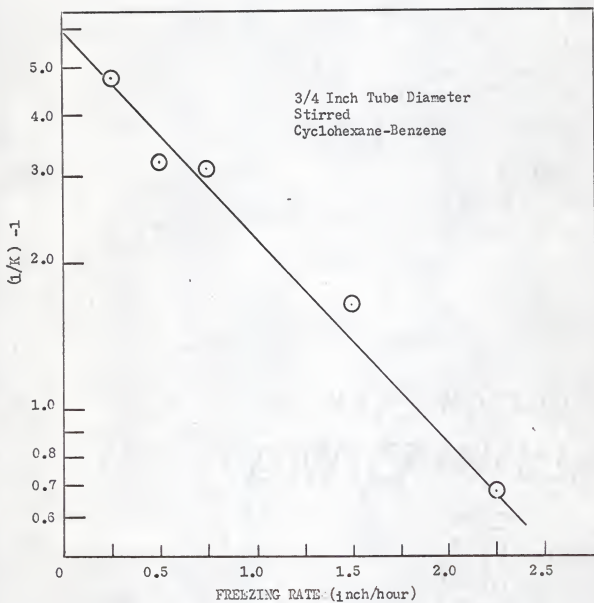
Fig. 17. LOG((1/K$_E$) -1) versus freezing rate.
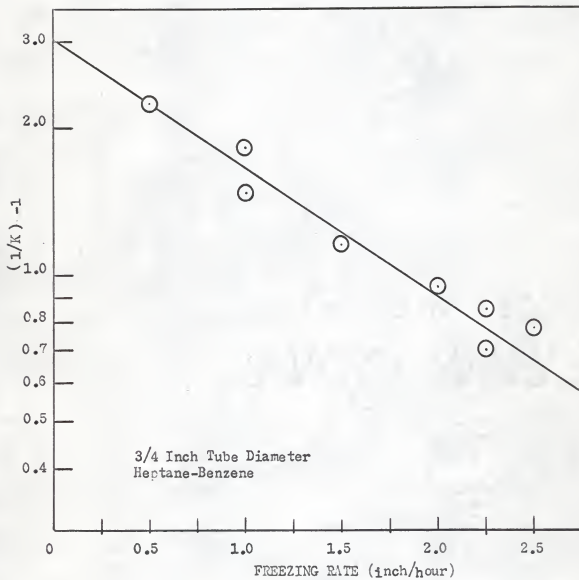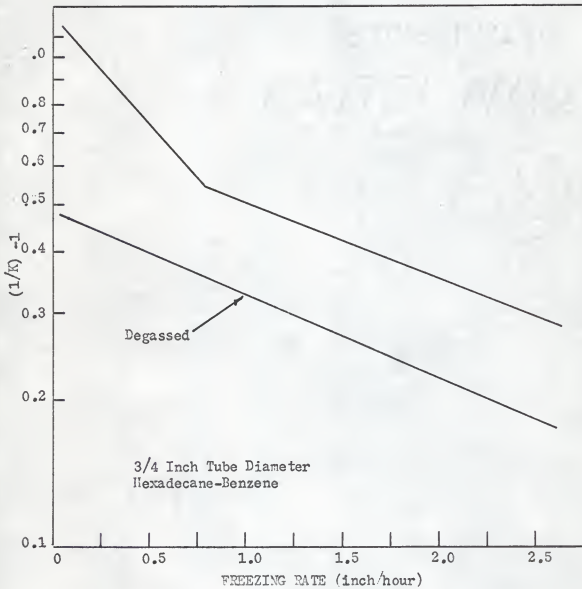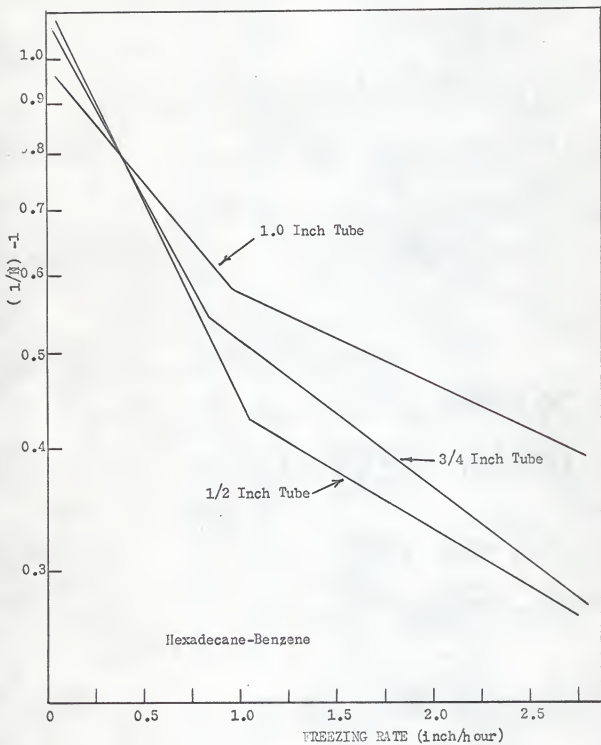
Fig. 18. LOG $((1/K_E) -1)$ versus freezing rate.
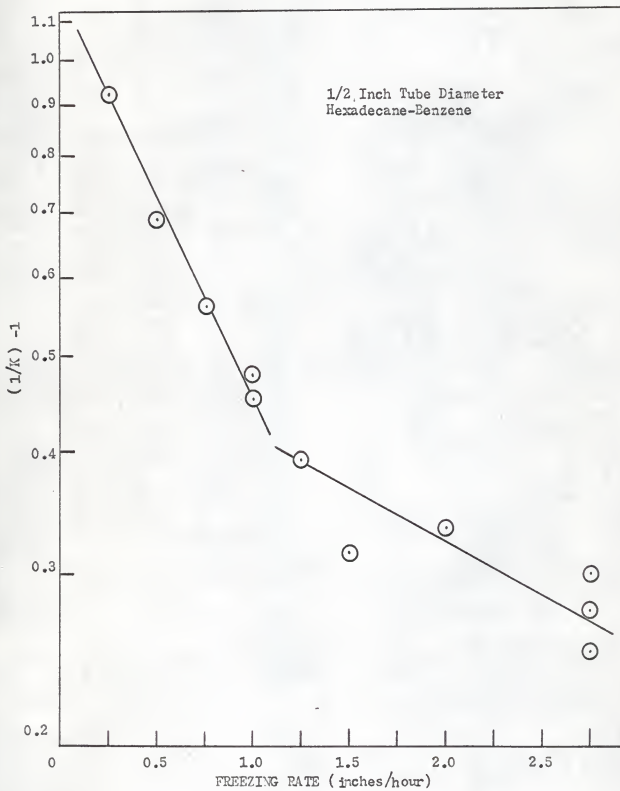
Fig. 19.   LOG((1/K_E) -1) versus freezing.
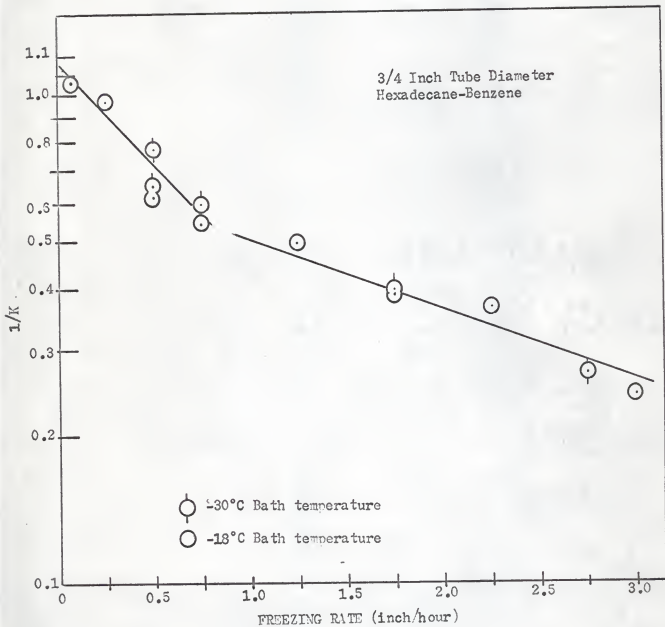
Fig. 20   LOG ((1/K_E) -1) versus freezing rate.
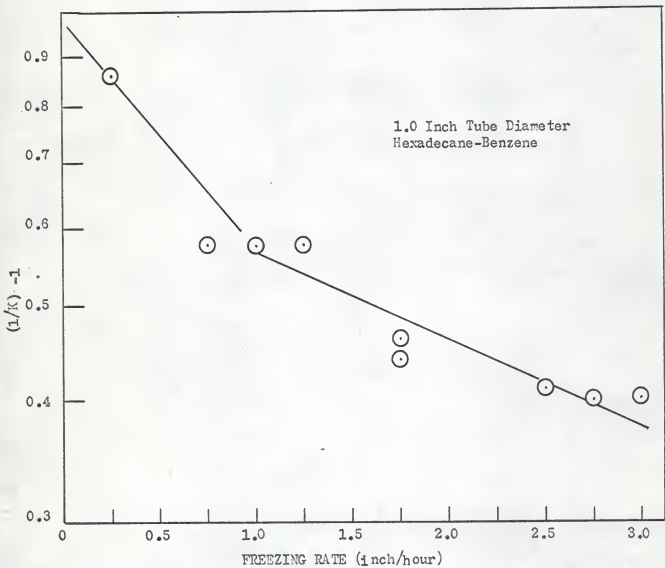
Fig. 21. LOG((1/K_E) -1) versus freezing rate.
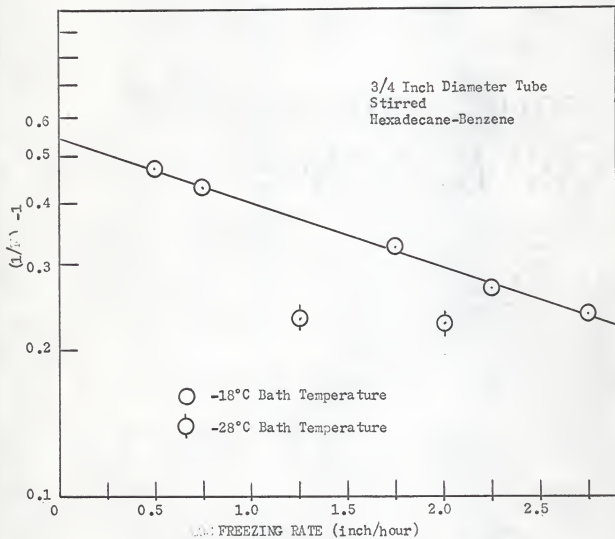
Fig. 22. LOG $((1/K_E) -1)$ versus freezing rate.
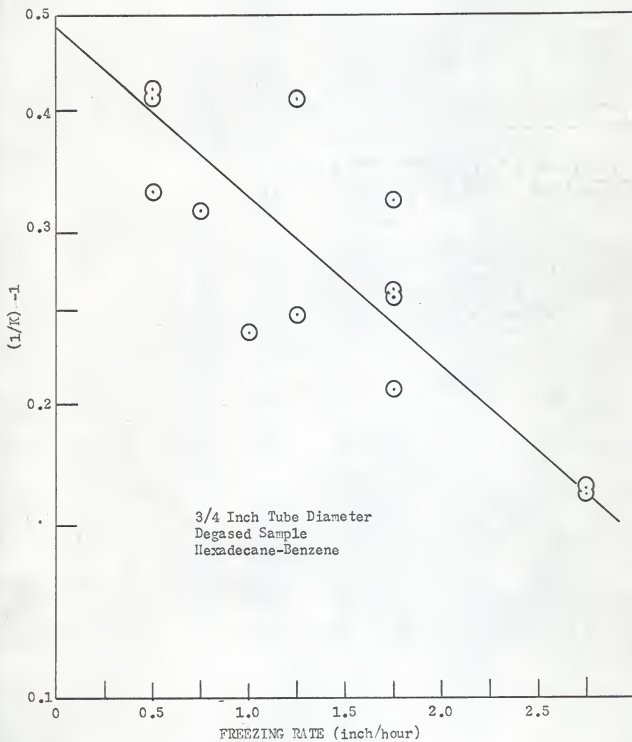
Fig. 23. LOG ((1/K_E) -1) versus freezing rate.
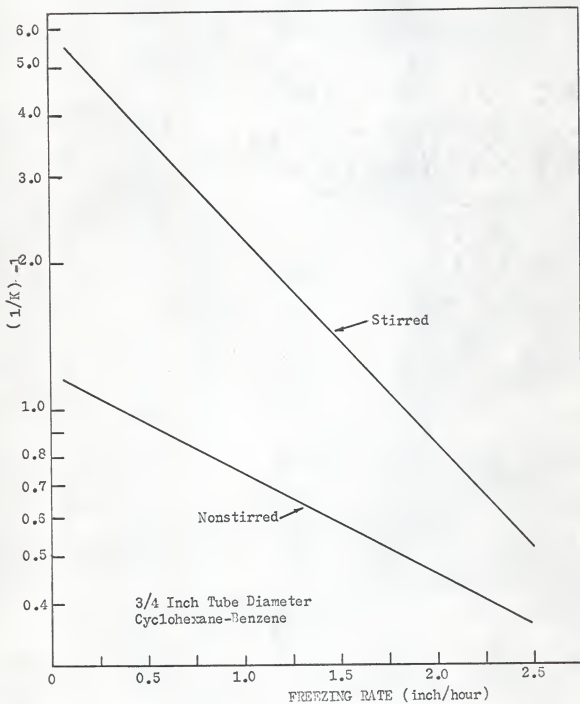
Fig. 24. LOG((1/K_E) -1) versus freezing rate.
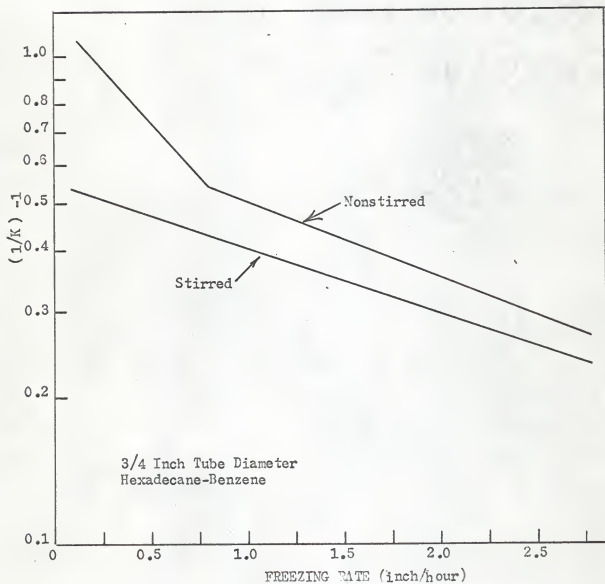
Fig. 25. LOG((1/K_E) -1) versus freezing rate.

Fig. 26. LOG ((1/k) -1) versus freezing rate.

Fig . 27 LOG$((1/K_E)$ -1) versus freezing rate.
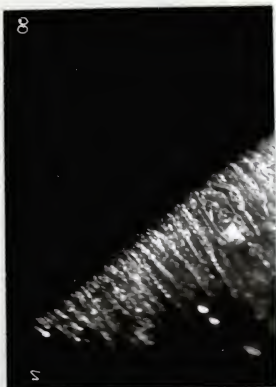
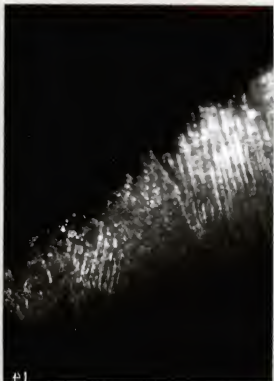PROFILE OF INTERFACE

hexadecane-benzene
rate: 0.50 in./hr.

PLATE No. 1

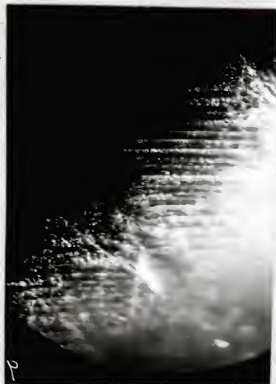PROFILE OF INTERFACE

hexadecane-benzene
rate: 0.75 in./hr.

PLATE No. 2

PROFILE OF INTERFACE

hexadecane-benzene
rate: 1.0 in./hr.

PLATE No. 3

PROFILE OF INTERFACE

hexadecane-benzene
rate: 1.25 in./hr.

PLATE No. 4

PROFILE OF INTERFACE

hexadecane-benzene
rate: 2.75 in./hr.

PLATE No. 5

PROFILE OF INTERFACE

benzene

PLATE No. 6

ACKNOWLEDGMENT

REFERENCES

1. Pfann, W. G., J. Metals, $\underline{4}$, 747 (1952).

2. Tiller, W. A., Jackson, K. A., Rutter, J. W., and Chalmers, B., Acta Met., $\underline{1}$, 428 (1953).

3. Smith, V. G., Tiller, W. A., and Rutter, J. W., Can. J. Phys., $\underline{33}$, 723 (1955).

4. Burton, J. A., Prim, R. C., and Slichter, W. P., J. Chem Phy., $\underline{21}$, 1987 (1953).

5. Wilcox, W. R., J. Appl. Phys., $\underline{35}$, 636 (1964).

6. Rutter, J. W. and Chalmers, B., Can. J. Phys., $\underline{31}$, 15 (1953).

7. Kyle, B. G., unpublished data.

8. Tiller, W. A. and Rutter J. W., Can. J. Phy., $\underline{34}$, 96 (1956).

9. Rutter, J. W. and Chalmers, B., Can. J. Phys., $\underline{31}$, 15 (1953).

10. Boiling, G. F. and Tiller, W. A., J. Appl. Phy., $\underline{31}$, 2040 (1960).

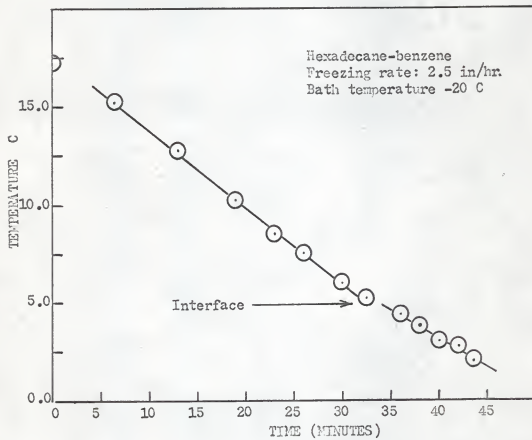11. Wilke, C. R. and Chang P., A. I. Ch. E. J., $\underline{1}$, 270 (1955).

APPENDICES
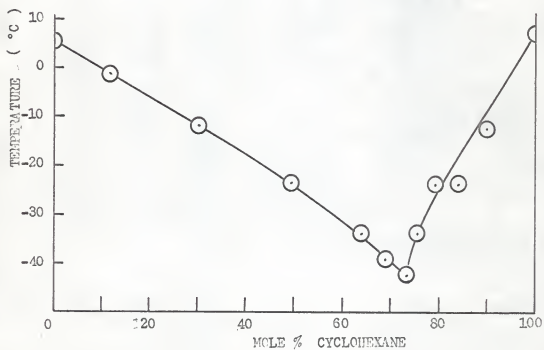
Appendix (1)

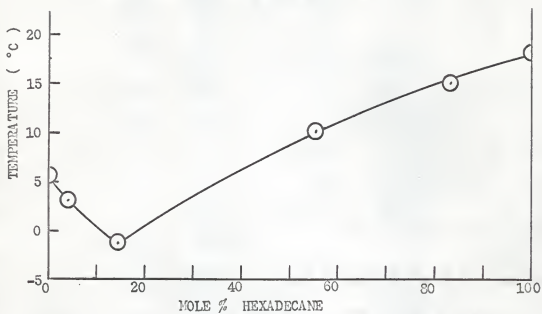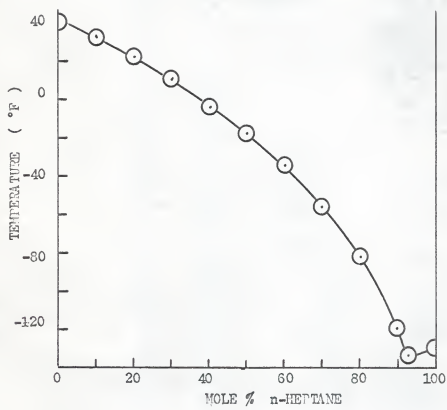Refractive index curve for hexadecane in benzene.
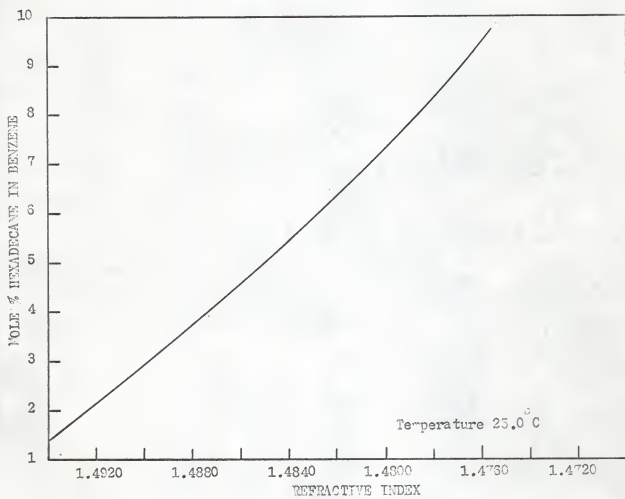
Appendix (2)

Temperature profile.

Hexadecane-benzene
Freezing rate: 2.5 in/hr.
Bath temperature -20 C

Interface →

Appendix (3)

Phase diagrams of hexadecane-benzene, cyclohexane-benzene, and heptane-benzene.

TEMPERATURE (°F)

MOLE % n-HEPTANE

Appendix (4)

Wilcox's composition profile for eutectic systems (5) is given as:

$$\frac{\Phi}{\Phi_\ell} = \frac{e^{-n}}{e^{-b}}$$

Applying the following conditions:

$$\Phi = W/W_o \quad \text{at } n$$

$$\Phi_\ell = W_\ell/W_o \quad \text{at bulk concentration}$$

Gives

$$C = C_\ell \, e^{-n+b}$$

Substituting for n and b gives

$$C = C_\ell \, e^{-(x' - \delta)\frac{f}{D}}$$

Using this value of the concentration gives the equilibrium temperature as:

$$T_E = T_o - mC_\ell \, e^{-(x' - \delta)\frac{f}{D}}$$

Taking the derivative with respect to x gives:

$$\left(\frac{dT_E}{dx'}\right)_{x'=0} = \frac{f}{D} m C_\ell \, e^{\frac{\delta f}{D}}$$

For constitutional subcooling to exist:

$$\frac{dT}{dx'} = G$$

After rearranging this gives:

$$\frac{G}{mC_\ell} = \frac{f}{D} e^{\frac{\delta f}{D}}$$

NORMAL FREEZING OF ORGANIC LIQUIDS

by

DAVID ARTHUR IRVIN

B. S., San Jose State College, 1964

————————————

AN ABSTRACT OF A MASTER'S THESIS

submitted in partial fulfillmet of the

requirements for the degree

MASTER OF SCIENCE

Department of Chemical Engineering

KANSAS STATE UNIVERSITY
Manhattan, Kansas

1965

Theoretical correlations predicting the segregation obtained by normal freezing of binary systems have been derived for both solid solutions and eutectic-forming mixtures by other investigators. It has been observed in metal systems that these correlations do not accurately predict segregation. It is believed the poor agreement is due to trapping of the liquid within the solid phase. This trapping is in turn believed caused by a phenomena called constitutional subcooling.

The composition profiles presented in this thesis were obtained for binary organic systems. The expression derived by Wilcox to apply to just such systems (simple eutectic) failed to predict the degree of segregation. It was found that a good correlation was obtained with Burton, Prim and Slichter's incomplete mixing boundary layer model even though it was derived for solid solution type systems. The effect of mixing in the liquid phase, tube diameter, and bath temperature tend to support the boundary layer model. Furthermore, it was noted that for the three organic systems investigated the calculated thickness for the boundary layer appeared not to vary a significant amount as required by boundary layer theory. The failure of the equations applying to eutectic systems is thought due to constitutional subcooling. It was found that the entire spectrum of freezing

rates investigated were subject to constitutional subcooling effects. From photographic studies of the interface two types of interfacial geometries were identified, a dendritic and a corrigated interface. The change from one form to the other appeared to occur at a freezing rate of 1.0 in/hr, with the dendritic form occuring at rates greater than 1.0 in/hr. The graphical representation of the data showed a discontinuity to occur at approximately the same rate as the transition in interfacial morphology (1.0 in/hr). The discontinuity is thought due to increased liquid trapping caused by the dendritic nature of the interface.